

Jin Lin, Xingcai Zhu, Kun Yang* and Jinhui Peng

Optimization of Microwave-Assisted Oxidation Roasting of Oxide–Sulphide Zinc Ore with Addition of Manganese Dioxide Using Response Surface Methodology

<https://doi.org/10.1515/htmp-2017-0184>

Received December 15, 2017; accepted July 30, 2018

Abstract: The present study deals with a microwave-assisted oxidation roasting oxide–sulphide zinc ore technology of with addition of manganese dioxide. Effects of roasting parameters such as MnO_2 addition level, roasting temperature, and holding time are studied by using the Central Composite Design (CCD). Meanwhile, zinc calcines are characterized by phase compositions analyses (XRD), structure characteristics of minerals (FT-IR), micro-area chemical analyses (SEM-EDAX) and elemental valence bonding analyses (XPS), which prove to be in accordance with the CCD results. The optimum roasting conditions are decided as MnO_2 addition level being 85.14 %, roasting temperature 680 °C, and holding time 41 mins, and oxidation degree of zinc can reach 88.22 %. Besides, when MnO_2 addition level reaches a certain value, zinc will aggregate in a form of $ZnMn_2O_4$, one battery material.

Keywords: Oxidation roasting, Oxide–sulphide zinc ore, Response surface methodology, MnO_2 addition

Introduction

With increasing scarce supply of non-ferrous metal resources, research on efficient utilization of non-traditional metal resources, such as oxide–sulphide zinc ore, is urgent [1, 2]. The oxide–sulphide zinc ore has a considerable reserve, intricate composition and complex mineralogy, thus it can't be ineffectively processed by the existing technology [3].

MnO_2 can act as an additive catalyst, which has been demonstrated the value of strengthening oxidation roasting, meanwhile fixing sulfur and suppressing emission of sulfur-containing flue gas [4]. Li et al. [5] separated and recovered antimony from high arsenic-bearing flue dusts through selective oxidation using MnO_2 , in which the arsenic was removed through a volatilization, and antimony was oxidized to Sb_2O_4 staying in the roasted products. Zhang et al. [6] investigated the feasibility of oxidative degradation of toxic nitrocellulose acid wastewater using low-grade MnO_2 ore as a cheap oxidant and the simultaneous release of Mn^{2+} for preparation of electrolytic manganese metal, and proved that TOC removal was significantly correlated with the release of Mn. It also can be referred that MnO_2 displays a promising application prospect in oxidation roasting.

The response surface methodology (RSM) is a powerful technology, which can eliminate and lower the time consuming and expensive of “one factor at a time optimization approach” [7, 8], via a minimum number of experimental trials by a Central Composite Design (CCD). What's more, the CCD allows simultaneous optimization of conditions and identifies significant interactions among variables [9–11].

This work is devoted to optimizing microwave-assisted oxidation roasting of oxide–sulphide zinc ore with addition of manganese dioxide. CCD of RSM is employed to investigate the effect of significant operating parameters, including MnO_2 addition level, roasting temperature and holding time on oxidation degree of zinc ore to find the most suitable combination of variables to achieve a maximum phase transformation result.

*Corresponding author: Kun Yang, Faculty of Metallurgical and Energy Engineering, Kunming University of Science and Technology, Kunming, Yunnan 650093, China; State Key Laboratory of Complex Nonferrous Metal Resources Clean Utilization, Kunming, Yunnan 650093, China, E-mail: truepsyche@sina.com

Jin Lin, Engineering Training Center, Kunming, Yunnan 650093, China; Faculty of Metallurgical and Energy Engineering, Kunming University of Science and Technology, Kunming, Yunnan 650093, China; State Key Laboratory of Complex Nonferrous Metal Resources Clean Utilization, Kunming, Yunnan 650093, China

Xingcai Zhu, Materials & Metallurgy Chemical Engineering Department, Yunnan Tin Vocational& Technical College, Gejiu, Yunnan 661000, China

Jinhui Peng, Faculty of Metallurgical and Energy Engineering, Kunming University of Science and Technology, Kunming, Yunnan 650093, China; State Key Laboratory of Complex Nonferrous Metal Resources Clean Utilization, Kunming, Yunnan 650093, China

Materials and methods

Materials and reagents

The oxide-sulphide zinc is from a domestic lead and zinc smelter. Main chemical composition and mineralogical analysis of oxide-sulphide zinc ore are presented in Tables 1 and 2, respectively. Figure 1 gives the XRD pattern of raw ore. These detections affirm that this oxide-sulphide zinc ore consists of a large amount of ZnS, ZnCO₃, SiO₂ and CaCO₃, small amount of FeS₂, PbS and Zn₂SiO₄, and trace amounts of Fe₂O₃ and PbCO₃. All chemical reagents used for this experiment are analytical pure.

Table 1: Main chemical composition of oxide-sulphide zinc ore (mass fraction, wt%).

Zn	CaO	SiO ₂	S	Fe	Pb	Al ₂ O ₃	MgO
24.91	11.96	10.30	10.20	7.70	4.80	1.27	0.22

Table 2: Mineralogical analysis of oxide-sulphide zinc ore.

Zinc phase	ZnS	ZnCO ₃	Zn ₂ SiO ₄	ZnFe ₂ O ₄	Zn
Mass fraction/wt%	11.06	9.68	4.00	0.052	24.91
Distribution/wt%	44.61	39.04	16.13	0.21	100

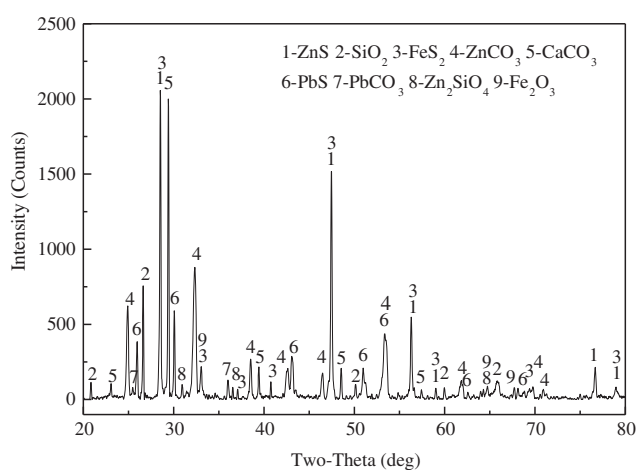


Figure 1: XRD pattern of oxide-sulphide zinc ore.

Instrumental analyses

The XRD patterns of samples are recorded in a Rigaku D/MAX-3B X-ray diffractometer with a detecting speed

of 4 deg/min. SEM-EDAX analyses obtains in a FEI Quanta 200 scanning electron microscope. The X-ray photoelectron spectroscopy (XPS) performs in a LAS-3000 surface analysis system (RIBER, France).

Process variables and design of experiments

Design-Expert is applied to build the matrix and generate the response surface models. A CCD with three levels and three factors is adopted in this study, as it can evaluate quadratic interactions between pairs of factors while minimizing the number of required experiments [12]. The influences and values of three factors examined include MnO₂ addition level, holding time and roasting temperature. 20 experiments with different factor values are performed. The response is measured for each experiment and the oxidation degree are evaluated based on an established mathematical model.

The microwave-assisted oxidation roasting of oxide-sulphide zinc ore with addition of manganese dioxide conducts as: mix zinc ore and MnO₂ at some mass ratio, then roast the mixture in a self-made high temperature microwave equipment according to the CCD design. After a period of constant temperature heating, characterize the zinc calcines.

Results and discussion

Fitting the process models

The 3-factor CCD matrix and experimental results obtained for the microwave-assisted oxidation roasting of oxide-sulphide zinc ore with addition of manganese dioxide are presented in Table 3, in which the correlation of oxidation degree (Y) with MnO₂ addition level (X_1), holding time (X_2) and calcination temperature (X_3) taken as variables is studied.

Regression equation

Following a polynomial regression model correlation, the mathematical relationship of oxidation degree with operating variables can be obtained as:

$$Y = 66.40 + 27.60 \cdot X_1 + 2.04 \cdot X_2 + 4.16 \cdot X_3 - 1.40 \cdot X_1 \cdot X_2$$

$$- 2.71 \cdot X_1 \cdot X_3 + 0.54 \cdot X_2 \cdot X_3 - 6.27 \cdot X_1^2 - 1.08 \cdot X_2^2 - 1.69 \cdot X_3^2$$

Table 3: Central composite design arrangement and results of microwave-assisted oxidation roasting of oxide–sulphide zinc ore with addition of manganese dioxide.

No.	MnO ₂ addition level (%)	Holding time (mins)	Roasting temperature (°C)	Oxidation degree (%)
1	85.14	49.87	709.46	87.72
2	55.26	35.00	750.00	70.03
3	55.26	35.00	650.00	66.01
4	55.26	35.00	650.00	67.12
5	105.52	35.00	650.00	93.81
6	25.38	20.13	590.54	17.48
7	85.14	20.13	709.46	85.42
8	5.00	35.00	650.00	6.87
9	25.38	49.87	590.54	23.24
10	55.26	35.00	650.00	64.94
11	85.14	20.13	590.54	83.41
12	55.26	35.00	550.00	56.58
13	85.14	49.87	590.54	83.46
14	55.26	35.00	650.00	66.72
15	55.26	60.00	650.00	68.58
16	55.26	10.00	650.00	61.44
17	55.26	35.00	650.00	68.18
18	25.38	49.87	709.46	38.22
19	25.38	20.13	709.46	30.42
20	55.26	35.00	650.00	64.85

Through a comparison of prediction values using the above equation with experimental values, it is found that, oxidation degree has R^2 value of 0.9942, which explains this model possesses a high fitting degree, and 99.42% of the experimental data can be explained.

Surface and contour plots

In the response surface optimization experiments, it needs to perform an accuracy analysis for the model, which is accomplished by a RSM experimental design. On the basis of regression and variance analysis, two-dimensional and three-dimensional response surfaces of the regression model are established. Response surface plots for MnO₂ adding level vs. roasting temperature vs. holding time corresponding to the optimized quadratic model (formula 1) is obtained as in Figure 2.

Figure 2 (a) illustrates the 3D response curves and contour for MnO₂ adding level vs. holding time. It can be seen that the oxidation rate is positively correlated with MnO₂ addition level and holding time, that is, with the increasing of MnO₂ level or holding time, oxidation rate will improve. Figure 2 (b) and (c) display same behaviors.

Optimization and verification

By the prediction function of response surface software, optimization is carried out to determine MnO₂ addition level, roasting temperature and holding time. The experimental results are compared with predicted values. Optimization process parameters of the regression mode are as Table 4.

Under conditions of optimized process parameters, the results (oxidation degree) of two parallel experiments are basically close to 88%, which verifies the reliability of optimization results.

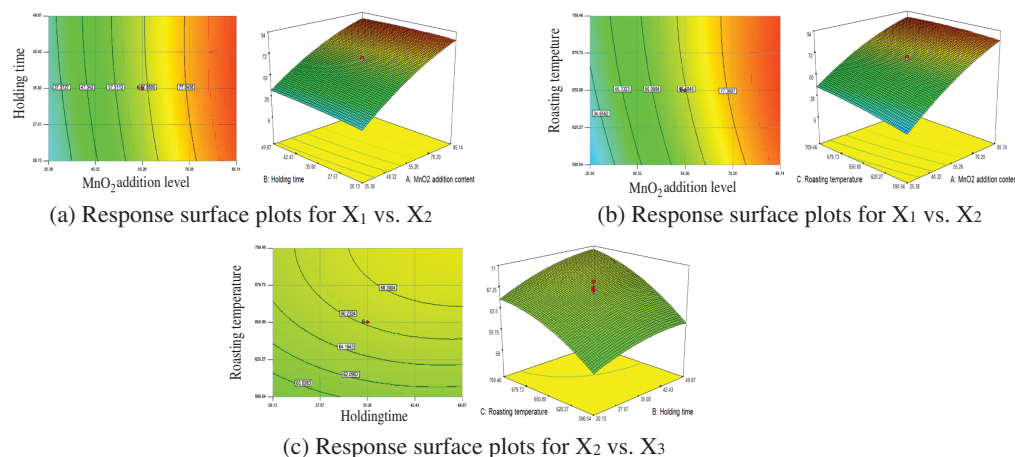


Figure 2: Response surface plots for MnO₂ adding level vs. holding time vs. roasting temperature. (a) Response surface plots for X₁ vs. X₂. (b) Response surface plots for X₁ vs. X₃. (c) Response surface plots for X₂ vs. X₃.

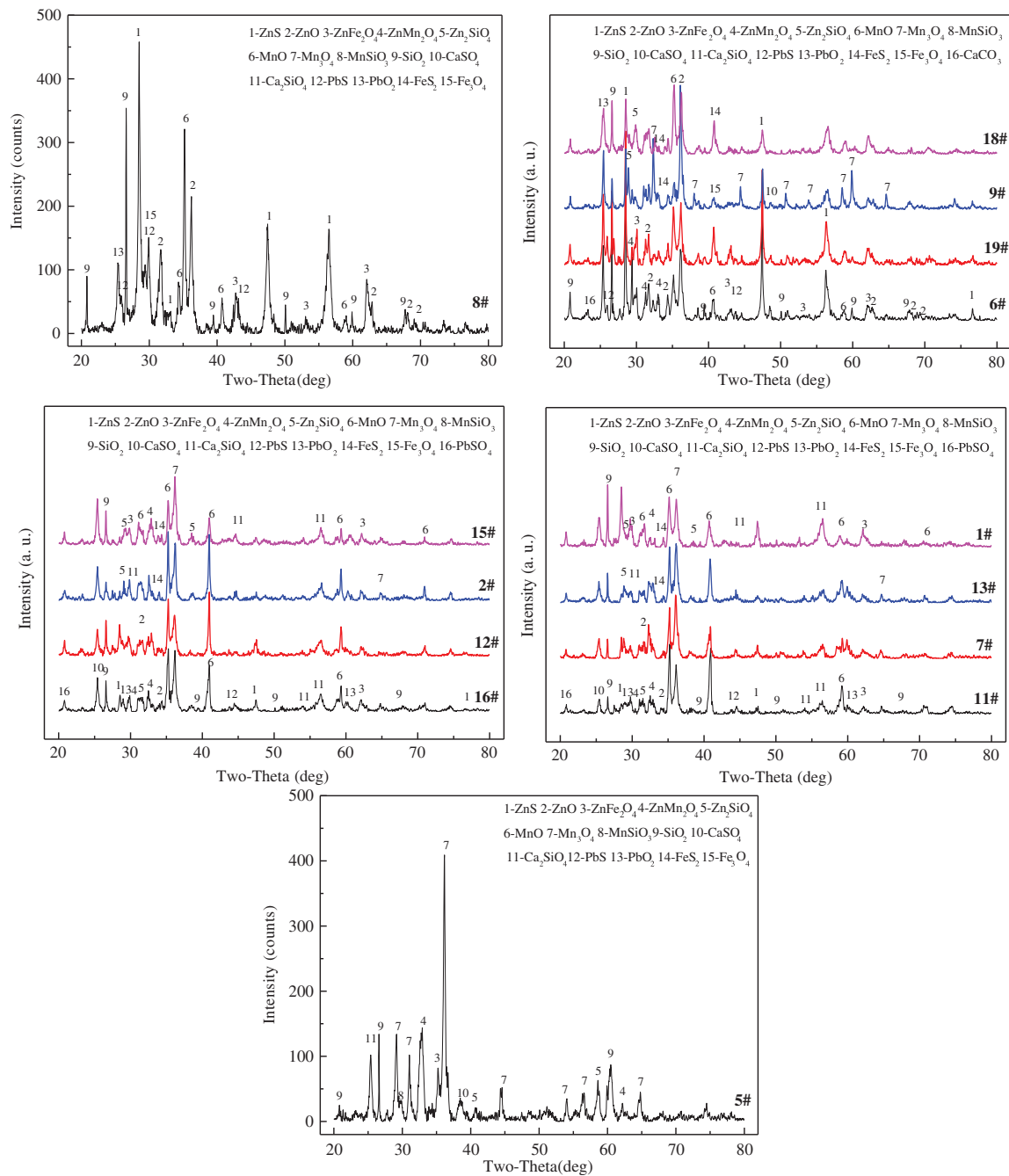
Table 4: Optimization process parameters of the regression model.

MnO ₂ addition level (%)	Holding time (mins)	Roasting temperature (°C)	Oxidation degree (%)	Desirability
85.14	41.21	679.49	88.22018	0.42122

Zinc calcines analyses

Phase compositions analyses

The XRD patterns of zinc calcines corresponding to Table 3 compare in Figure 3. As can be seen, MnO₂ addition level is

**Figure 3:** XRD patterns of zinc calcine.

the critical factor for microwave-assisted oxidation roasting of oxide–sulphide zinc ore. When MnO_2 addition level is 5 %, main phase of zinc exists as ZnS , and part exist as ZnO and ZnFe_2O_4 . Besides, MnO_2 has been reduced to MnO .

With further addition of MnO_2 , ZnMn_2O_4 forms. Main zinc-containing phases change to ZnS , ZnO and ZnFe_2O_4 , as adds 25.37 % MnO_2 . Besides, there also generate a little ZnMn_2O_4 and a new phase- Mn_3O_4 . After that, ZnMn_2O_4 and ZnFe_2O_4 domain, meanwhile MnO gradually transforms to Mn_3O_4 . Thus, the reaction with addition of MnO_2 can be deduced as, ZnS first oxidizes to ZnO , and then transforms to ZnMn_2O_4 with MnO . Compared to MnO_2 addition level, roasting temperature and holding time can be judged to be unobvious factors.

Structure characteristic of minerals

Figure 4 analyzes the structure characteristic of zinc calcines presented in Table 3.

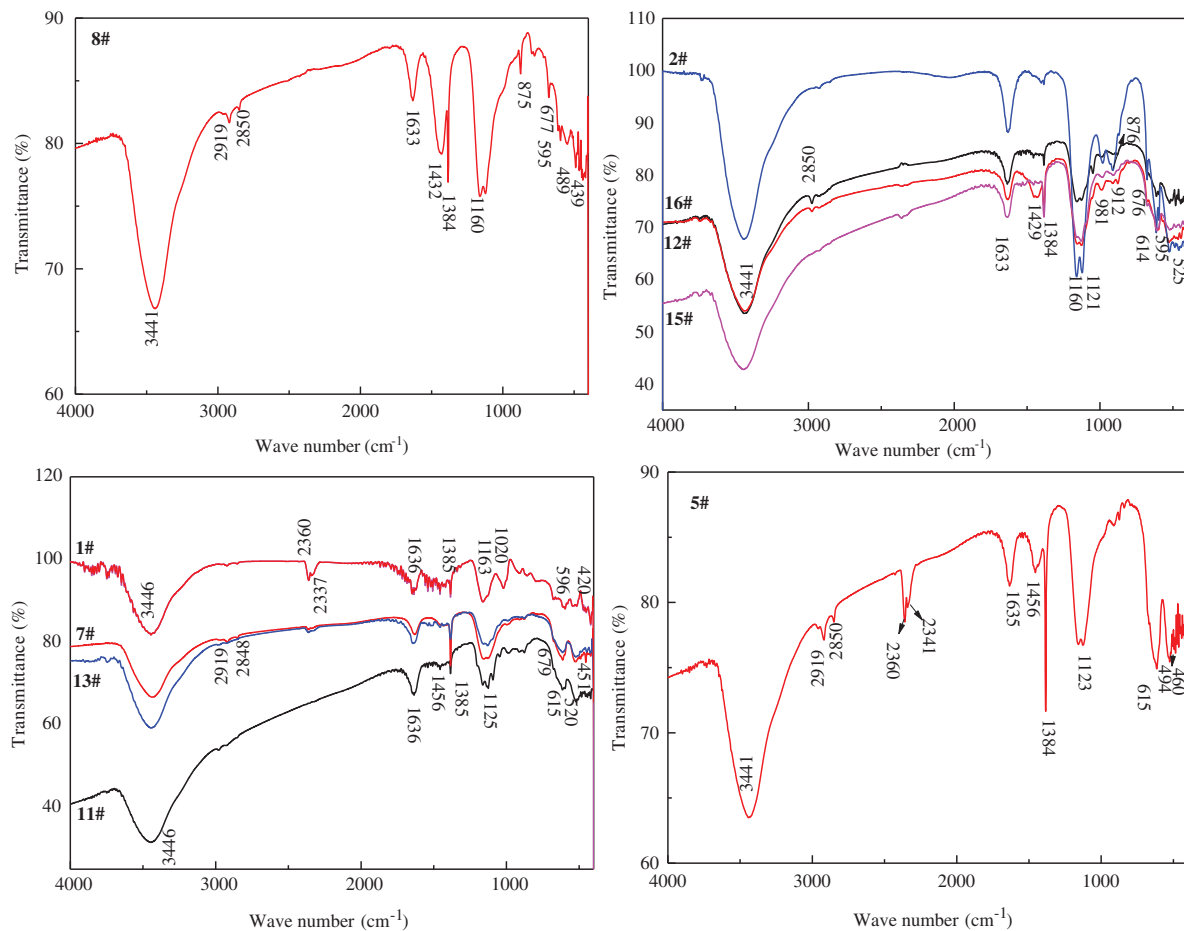


Figure 4: FT-IR spectra of zinc calcines.

It can be seen from the figures that main transmission peaks include 3441, 2919, 2850, 2341, 1635, 1456, 1384, 1123, 615 and 525 cm^{-1} . Wherein, 452 cm^{-1} is caused by Zn-O stretching vibration [13]. Vibration spectrum at 505, 614 and 677 cm^{-1} are attributed to Mn-O [14, 15], which also demonstrates the presence of ZnMn_2O_4 . No. 8 is the only one without spectra of ZnMn_2O_4 , and verifies the XRD detection results.

Micro-area chemical analysis

Micro-area chemical analysis is performed on No. 8 zinc calcine in Table 3, and result is shown in Figure 5, for which addition amount of manganese dioxide is 5 %, roasting temperature is 650 $^{\circ}\text{C}$, and holding time is 35 mins. According to the EDAX analyses and elemental distribution map scanning, there can divide three mineral zones in the observation horizon, zone 1# is the regional aggregation of MnO , ZnS , ZnO and PbS . Zone 2# is the coexistence area of MnO and ZnO , which appear as a fine dispersed state, and

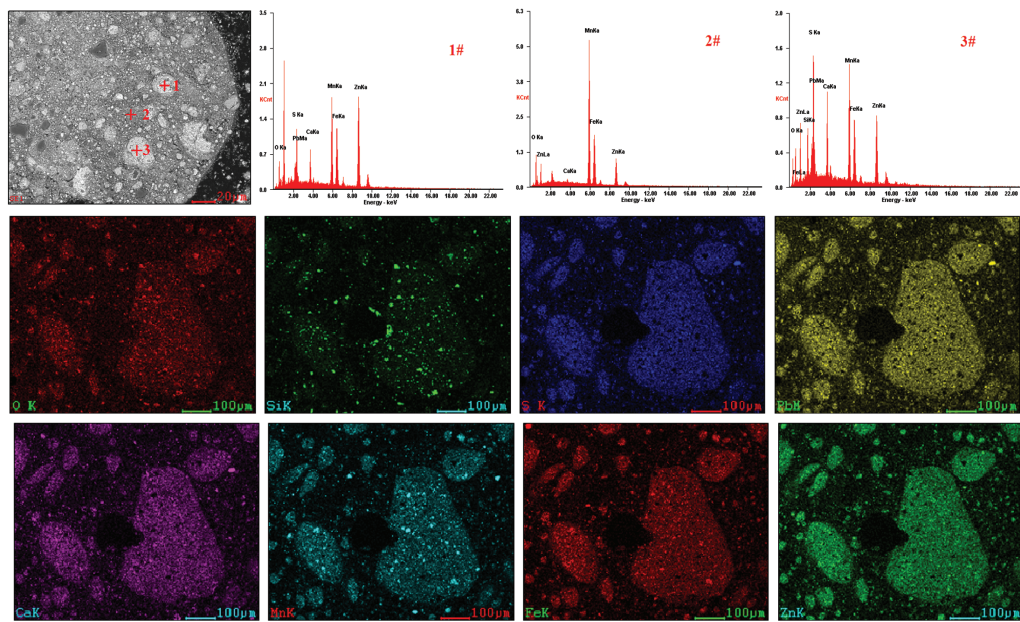


Figure 5: SEM-EDAX analysis of zinc calcine (No. 8).

their contents are not high. Mineral components of zone 3# are basically similar as 1#, while possess a higher content of sulphur and Si. Judging from the elemental distribution map scanning, Zn, Pb, Mn, Fe and S present in a substantially uniform state, and elemental symbiosis phenomena will not occur, while SiO_2 remains aggregate separately.

The zinc calcine (NO. 5) in Figure 6 obtains under conditions of MnO_2 addition level being 105.52 %,

roasting temperature 650°C , and holding time 35 mins, in which a phenomenon of melt aggregation emerges. EDAX results prove ZnMn_2O_4 is the eutectic of ZnO , MnO and MnO_2 , which is consistent with the results of XRD analysis. Furthermore, Mn, O and Zn will accumulate together, that is, ZnMn_2O_4 , and Ca, S and O form a CaSO_4 symbiont. A small amount of PbSO_4 also presents.

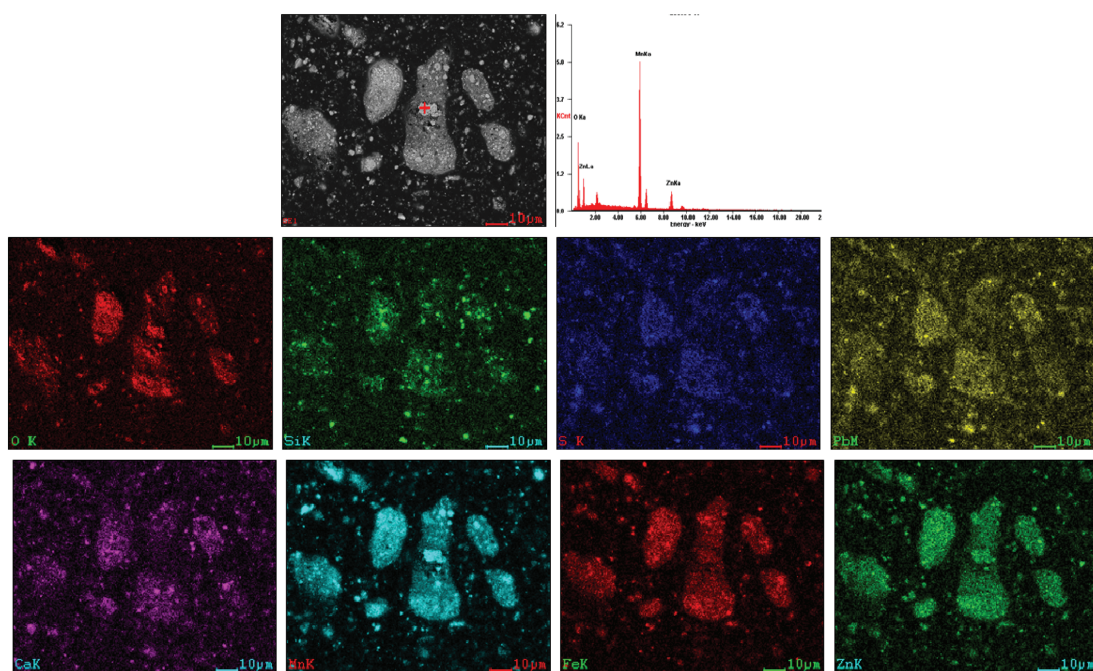


Figure 6: SEM-EDAX analysis of zinc calcine (No. 5).

Elemental valence bonding analysis

The XPS detail spectra of S and Mn are shown in Figure 7. S2p diffraction peaks can be divided into two energy bands, ~ 168 eV attributed to high value

sulphates, and ~ 160 eV attributed to low value sulphide [16, 17]. Through comparing, content of high value sulphate increases with gradually doping MnO_2 . When the doping level reaches 55.26 %, there just exists a low amount of S^{2-} .

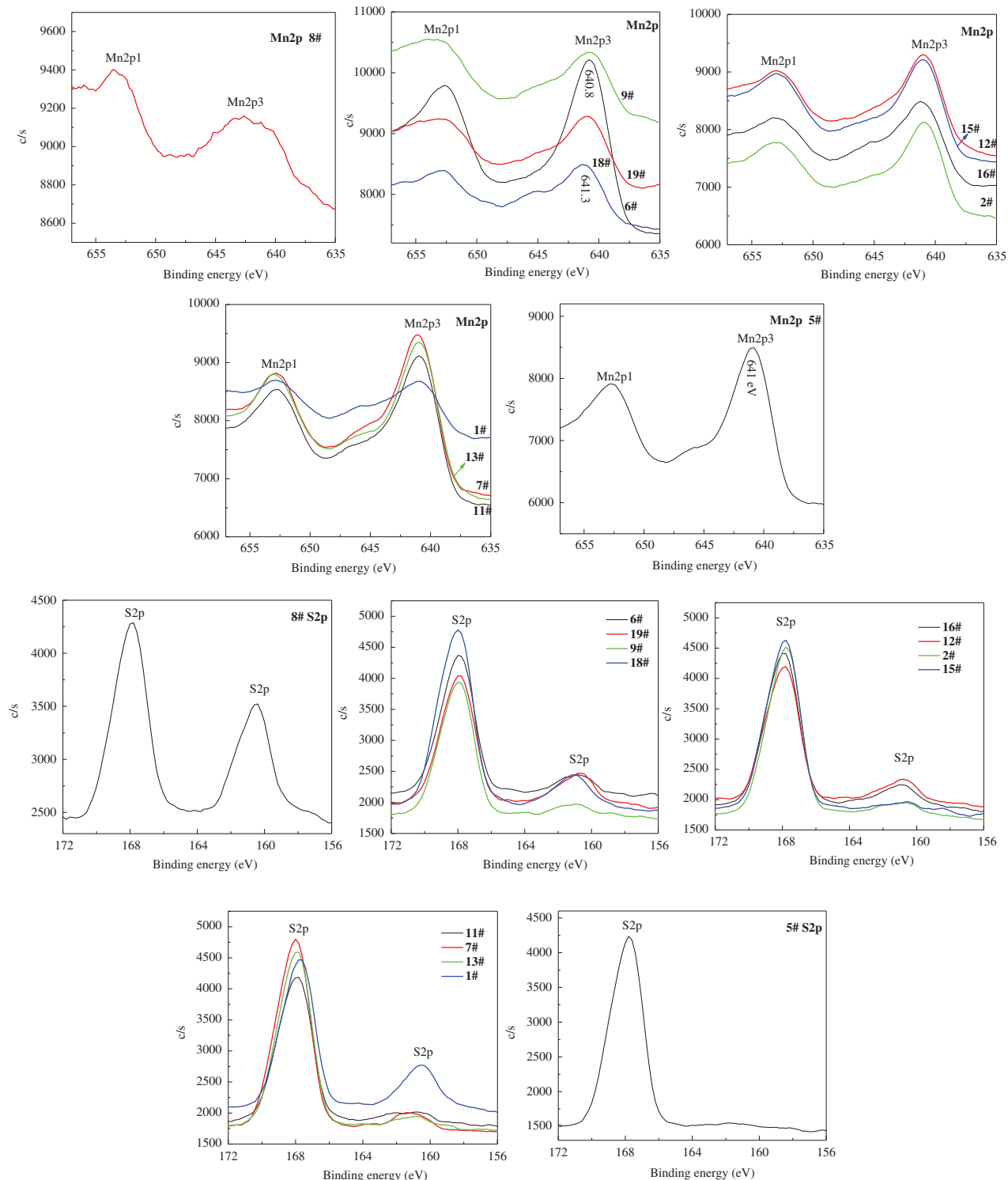


Figure 7: XPS detail spectra of S and Mn in zinc calcine with different MnO_2 level.

Umezawa and Reilley [18] reported that the Mn2p3 peak of MnO₂ is at 643.4 eV. Mn2p3 valence band energy of MnFe₂O₄, CuMn₂O₄ and Mn₃O₄ is at 641.0 eV [19–21]. Mn2p3 peak between 640.7 eV and 641 eV belongs to the MnO [22, 23]. According to the reported data, increasing amount of MnO₂ will render Mn2p spectrum shift to high value, namely, MnO transforms to ZnMn₂O₄.

Conclusions

In this paper, reaction mechanism of microwave-assisted oxidation roasting of oxide–sulphide zinc ore with addition of MnO₂ is discussed, and optimum roasting conditions are decided by exploiting response surface methodology, and ascertained by microscopic analysis. Results show that,

The optimized conditions for this design are MnO₂ addition level being 85.14 %, roasting temperature 680 °C, and holding time 41 mins, and oxidation degree of zinc can reach 88.22 %.

When MnO₂ addition level reaches a certain value, aggregation phenomenon of zinc appears, and content of S obviously decreases. According to the EDAX analysis, appearance of ZnMn₂O₄ is confirmed.

Acknowledgements: This work is supported by Project supported by the National Program on Key Basic Research Project of China (973 Program, 2014CB643404) and Yunnan Provincial Department of Education Science Research Fund Project (2016zzx291).

References

- [1] D. Yang, H. Zhu and J. Chen, *Hydrometallurgical Zinc Process and Technology*, Metallurgical Industry Press, Beijing (2006).
- [2] K. Yang, S. Li, L. Zhang, J. Peng, W. Chen, F. Xie and A. Ma, *Hydrometallurgy*, 166 (2016) 243–251.
- [3] K. Yang, L. Zhang, X. Zhu, J. Peng, S. Li, A. Ma, H. Li and F. Zhu, *J. Hazard. Mater.*, 343 (2018) 315–323.
- [4] Y. Zhu, C. Liu, Q. Yang, P. Li, Y. Sun and D. Xu, *Adv. Mat. Res., Trans. Tech. Publ.*, 773 (2013) 634–638.
- [5] L. Li, F. Wang, D. Zhong, C. Tan and Y. Yu, *ISIJ Int.*, 57 (2017) 581–586.
- [6] Y. Zhang, J. Cai, Z. Dan, Y. Tian, N. Duan and B. Xin, *J. Chem. Technol. Biot.* (2017).
- [7] A. Asfaram, M. Ghaedi, A. Goudarzi and M. Rajabi, *Dalton T.*, 44 (2015) 14707–14723.
- [8] S. Chowdhury, S. Chakraborty and P.D. Saha, *Environ. Sci. Pollut. R.*, 20 (2013) 1698–1705.
- [9] P. Das, P. Banerjee and S. Monda, *Environ. Sci. Pollut. R.*, 22 (2015) 1318–1328.
- [10] A. Asfaram, M. Ghaedi, S. Agarwal, I. Tyagi and V.K. Gupta, *RSC Adv.*, 5 (2015) 18438–18450.
- [11] F. Priscila, Z.M. Magriots, M.A. Rossi, R.F. Resende and C.A. Nunes, *J. Environ. Manage.*, 130 (2013) 417–428.
- [12] M.W. Amer, R.A. Ahmad and A.M. Awwad, *Int. J. Ind. Chem.*, 6 (2015) 67–75.
- [13] L. Zhang, H. Cheng, R. Zong and Y. Zhu, *J. Phys. Chem. C*, 113 (2009) 2368–2374.
- [14] P.K. Sharma and M.S. Whittingham, *Mater. Lett.*, 48 (2001) 319–323.
- [15] Z. Bai, N. Fan, C. Sun, Z. Ju, C. Guo, J. Yang and Y. Qian, *Nanoscale*, 5 (2013) 2442–2447.
- [16] T.N. Khmeleva, W. Skinner and D.A. Beattie, *Int. J. Miner. Process.*, 76 (2005) 43–53.
- [17] A. Parker, C. Klauber, A. Kougianos, H.R. Watling and W. Van Bronswijk, *Hydrometallurgy*, 71 (2003) 265–276.
- [18] Y. Umezawa and C.N. Reilley, *Anal. Chem.*, 50 (1978) 1290–1295.
- [19] V.A.M. Brabers, F.M. Van Setten and P.S.A. Knapen, *J. Solid State Chem.*, 49 (1983) 93–98.
- [20] M. Oku and K. Hirokawa, *J. Electron. Spectrosc.*, 8 (1976) 475–481.
- [21] B.R. Strohmeier and D.M. Hercules, *J. Phys. Chem.*, 88 (1984) 4922–4929.
- [22] M. Oku, K. Hirokawa and S. Ikeda, *J. Electron. Spectrosc.*, 7 (1975) 465–473.
- [23] A. Aoki, *Jpn. J. Appl. Phys.*, 15 (1976) 305.